DEVELOPMENTAL DYNAMICS 237:3842–3852, 2008

Identification and Expression of Voltage-Gated Calcium Channel β Subunits in Zebrafish

Weibin Zhou,[†] Eric James Horstick, Hiromi Hirata,[‡] and John Y. Kuwada*

Voltage-gated calcium channels (VGCC) play important roles in electrically excitable cells and embryonic development. The VGCC β subunits are essential for membrane localization of the channel and exert modulatory effects on channel functions. In mammals, the VGCC β subunit gene family contains four members. In zebrafish, there appear to be seven VGCC β subunits including the previously identified β1 subunit. cDNAs for six additional VGCC β subunit homologs were identified in zebrafish, their chromosomal locations determined and their expression patterns characterized during embryonic development. These six genes are primarily expressed in the nervous system with *cacnb4a* also expressed in the developing heart. Sequence homology, genomic synteny and expression patterns suggest that there are three pairs of duplicate genes for β2, β3, and β4 in zebrafish with distinct expression patterns during embryonic development. *Developmental Dynamics 237:3842–3852, 2008.* © 2008 Wiley-Liss, Inc.

Key words: zebrafish; voltage-gated calcium channel; CACNB; spinal cord; nervous system; Rohon-Beard neuron; trigeminal ganglion; lateral line ganglion; heart; retina; VGCC

Accepted 10 September 2008

INTRODUCTION

Voltage-gated calcium channels (VGCC) mediate Ca^{2+} influx into cells upon activation by membrane depolarization (Catterall, 2000). In excitable cells, such as muscles, neurons and endocrine cells, voltage-gated calcium channels play important roles in a variety of processes, including excitation–contraction coupling, synaptic transmission, and hormone secretion (Sheng et al., 1994; Rettig et al., 1997; Schredelseker et al., 2005). In addition, Ca^{2+} entering through voltage-gated calcium channels can serve as a second messenger in signaling pathways to regulate gene expression in developmental processes, including mesoderm patterning, neural induction, process outgrowth, neuronal migration, and cardiac cell differentiation (Komuro and Rakic, 1992; Moorman and Hume, 1993; Moreau et al., 1994; Leclerc et al., 1995, 1997, 2000; Brosenitsch et al., 1998; Haase et al., 2000; Palma et al., 2001; Rottbauer et al., 2001).

Each VGCC usually consists of a pore-forming α1 subunit, a cytoplasmic β subunit, an extracellular α2 subunit associated with a transmembrane δ subunit, and a transmembrane γ subunit (Dolphin, 2003). The α1 subunit contains four repeated domains, each having six transmembrane segments, which is sufficient to form the voltage-dependent Ca^{2+} channel. Among the auxiliary subunits, the β subunit modulates membrane targeting and the electrophysiological properties of the channel (Castellano et al., 1993; Herlitze et al., 2003). Coexpression of the β subunit with the α1 subunit is able to increase membrane expression and modify the pharmacological and biophysical properties of the channel (Bichet et al., 2000). How β subunits modulate these properties depends on the combination of α1 and β subunit types. For example, β subunits facilitate the voltage-dependence of the activation of L-type VGCCs but not non-L-type VGCCs. On the other hand, β subunits cause a hyperpolarizing shift of the inactivation of non-L-type VGCCs but not L-type VGCCs (Walker and De Waard, 1998).

Department of Molecular, Cellular and Developmental Biology, University of Michigan, Ann Arbor, Michigan
[†]Dr. Zhou's present address is Department of Pediatrics, University of Michigan Medical School, Ann Arbor, MI 48109-5646.
[‡]Dr. Hirata's present address is Division of Biological Science, Nagoya University, Furo-cho, Chikusa-ku, Nagoya 464-8602, Japan.
***Correspondence to: John Y. Kuwada, Graduate School of Science, University of Michigan, Department of Molecular Cellular and Developmental Biology, University of Michigan, Ann Arbor, MI 48109-1048. E-mail: kuwada@umich.edu**

DOI 10.1002/dvdy.21776
Published online 26 November 2008 in Wiley InterScience (www.interscience.wiley.com).

In mammals, there are four VGCC β subunit genes, *CACNB1-CACNB4* (Birnbaumer et al., 1998). Each VGCC β subunit protein (CAB) has five distinctive domains (D1–D5). D2 is a SH3 (Src Homology 3) -like domain and D4 is a MAGUK-like domain, which are found in the members of the membrane associated guanylate kinase (MAGUK) protein family (Dolphin, 2003). These two domains are highly conserved among CABs in different species. A motif at the beginning of D4 domain, known as β interaction domain (BID), is also highly conserved in all known VGCC β subunits and critical for the interaction between the VGCC α1 and β subunits. In contrast, D1, D3, and D5 are more variable.

Only a few nonmammalian *CACNB* genes have been identified (Dolphin, 2003). Recently the *cacnb1* gene was identified in zebrafish (Schredelseker et al., 2005; Zhou et al., 2006). The loss of function of zebrafish *cacnb1* causes the immotile phenotype of the zebrafish *relaxed* mutant, demonstrating the essential role of this gene for normal muscle function. Zebrafish *cacnb1* is expressed in skeletal muscle and the nervous system, in agreement with its mammalian orthologs, but no obvious defect in motor output from the central nervous system (CNS) was detected by electrophysiological recordings of skeletal muscle after sensory stimulation of *relaxed* embryos (Zhou et al., 2006). This raises the possibility that other members of the VGCC β subunit family may compensate for the loss of *cacnb1* in the nervous system of *relaxed* embryos as other β subunits are able to partially restore VGCC function in β1-deficient muscle in mammals (Beurg et al., 1999).

As an initial step toward the characterization of signaling within zebrafish neural circuits, we identified six additional zebrafish *CACNB* homologs by a sequence homology search of the zebrafish expressed sequence tag (EST) and genome databases. These *CACNB* homologs encode proteins that share the same domain structures with mammalian CABs and are mainly expressed in the nervous system with *cacnb4a* also expressed in the embryonic heart. The expression patterns within the nervous system of *CACNB* genes overlap with that of *cacnb1* suggesting that they may compensate for the loss of function of *cacnb1* in the nervous system of *relaxed* mutants.

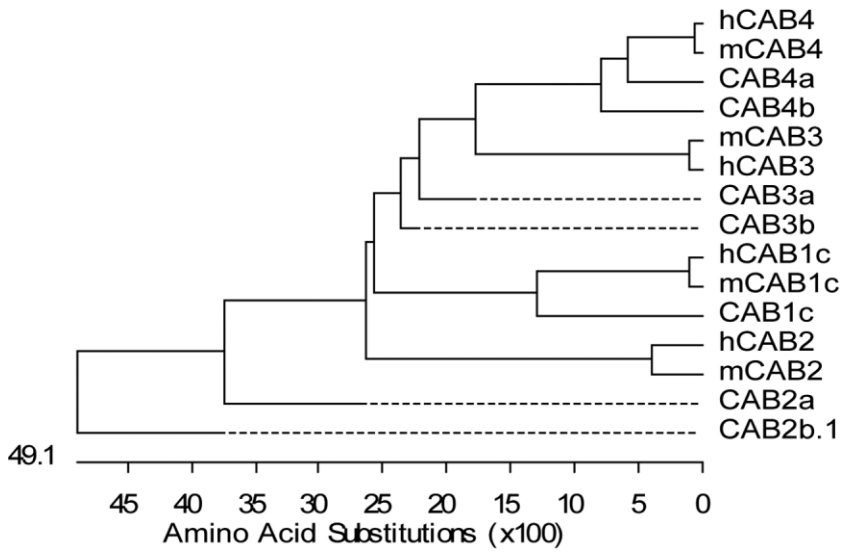

Fig. 1. Phylogenetic relationship of voltage-dependent calcium channel β subunits in zebrafish, mice, and human. Analysis of the protein sequence of zebrafish voltage-gated calcium channel (VGCC) β subunits with human and mouse VGCC β subunit protein (CAB) suggest that genes encoding CAB2, CAB3, and CAB4 are duplicated in zebrafish. Based on the phylogenetic distances, these zebrafish proteins are named CAB2a, CAB2b, CAB3a, CAB3b, CAB4a, and CAB4b and the corresponding genes *cacnb2a*, *2b*, *3a*, *3b*, *4a*, and *4b*. Human and mouse β subunits are denoted as hCABs and mCABs, respectively.

RESULTS AND DISCUSSION

We queried the EST (http://www.ncbi.nlm.nih.gov) and zebrafish genomic (http://www.ensembl.org/Danio rerio/) databases with the sequence of zebrafish *cacnb1c* (GenBank accession no. DQ198172) and identified six additional homologous sequences from zebrafish. The predicted protein sequences along with those of human and murine β subunits were aligned and analyzed phylogenetically to determine the relationship of the zebrafish genes to the mammalian counterparts (Fig. 1). The results suggested that the β2, β3, and β4 subunit genes were duplicated in zebrafish and thus they were named *cacnb2a* and *b*, *cacnb3a* and *b*, and *cacnb4a* and *b*.

Zebrafish *cacnb2a* and *cacnb2b*

We identified an EST clone (GenBank accession no. CN324195) for *cacnb2a* and complete sequencing of this EST (GenBank accession no. DQ372944) revealed that this cDNA encoded a protein of 377 amino acids that lacked most of the D5 domain. Mammalian *CACNB2* is alternatively spliced into many variants (Birnbaumer et al., 1998; Colecraft et al., 2002; Takahashi et al., 2003) including ones varying in the D1 domain that gave rise to distinct subcellular localizations and modulatory effects on L-type VGCC gating (Takahashi et al., 2003). However, no splice variant of β2 lacking the D5 domain was reported. Because the D5 domain is not required for interactions with the α1 subunit (Qin et al., 1997), the protein encoded by zebrafish *cacnb2a* could still bind the α1 subunit, but the physiological function of this β2 isoform is unknown.

The *cacnb2b* gene was identified from the zebrafish genome database in Zv6_scaffold1007 and Zv6_scaffold3352. Two cDNA sequences (GenBank accession no. DQ372945) for *cacnb2b* were cloned by reverse transcriptase-polymerase chain reaction (RT-PCR). *cacnb2b.1* encodes a protein (CAB2b.1) of 598 amino acids and *cacnb2b.2* encodes for an identical protein except that it has an in-frame deletion of 27 amino acids, suggesting that the two forms are derived from the same gene (Fig. 2A). Because the deletion disrupts the critical BID domain, the isoform encoded by *cacnb2b.2* is predicted not to interact

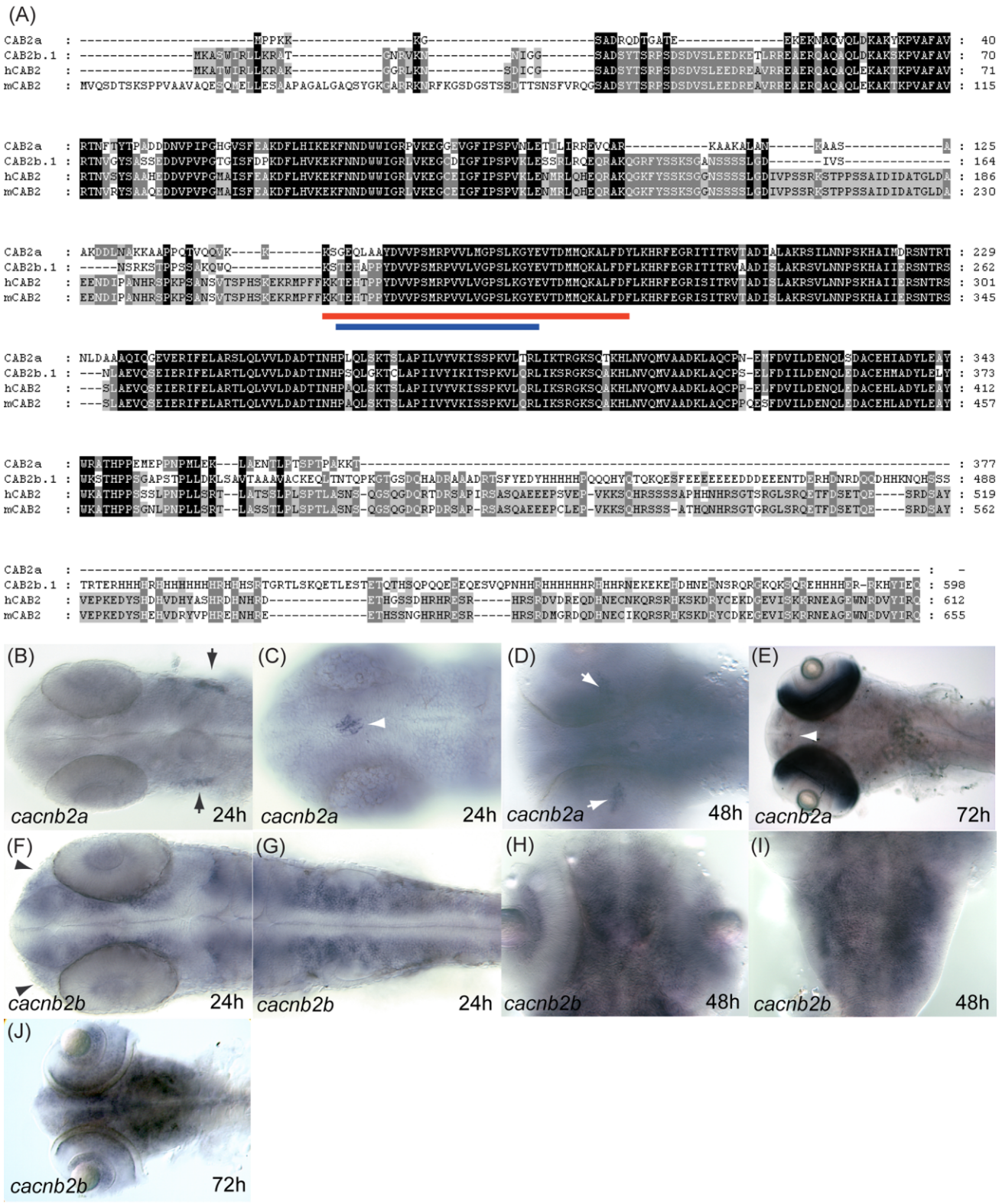

Fig. 2. Zebrafish *cacnb2a* and *cacnb2b* genes. **A:** Alignment of proteins encoded by zebrafish and mammalian *CACNB2* genes shows that they are highly homologous to each other. The red bar underlines the β interaction domain (BID). The blue bar underlines the deletion in the *cacnb2b.2* variant. **B:** Ventral view of the head region showing that *cacnb2a* is expressed in the trigeminal ganglion (arrows) at 24 hours post fertilization (hpf). **C:** View of the dorsal surface of the brain showing expression of *cacnb2a* in the epiphysis at 24 hpf. **D:** View of ventral surface of the brain showing strong expression of *cacnb2a* along the optic stalks (white arrows) and weaker expression in the brain at 48 hpf. **E:** Dorsal view of head region of a 72 hpf embryo showing expression of *cacnb2a* in the epiphysis (white arrowhead) and in the retina. **F:** Dorsal view showing that *cacnb2b* is expressed in the brain and olfactory placodes (arrowheads) at 24 hpf. **G:** Dorsal view showing that *cacnb2b* is expressed in the hindbrain and spinal cord at 24 hpf. **H:** Dorsal view showing that *cacnb2b* is strongly expressed in the brain and the retina at 48 hpf. **I:** Dorsal view showing that *cacnb2b* is expressed in the hindbrain at 48 hpf. **J:** Dorsal view of 72 hpf embryo showing strong *cacnb2b* expression in the brain. Anterior is left in all the panels except (H–I).

with VGCC α1 subunits. *cacnb2a* and *cacnb2b* are most closely related to mammalian *CACNB2* genes. The proteins encoded by these two genes (zebrafish CAB2a and CAB2b.1) have 50% and 67% similarity with human CAB2.

We determined the chromosomal location of the two genes by radiation-hybrid mapping. *cacnb2a* was mapped to Chromosome 2, 16.37cR from EST maker fc08d03 (LOD = 10.8) and *cacnb2b* to Chromosome 7 at the location of EST marker fa93e09 (LOD = 16.5). In the mouse and human genomes, the *CACNB2* gene is located close to the signal transducing adapter molecule (STAM) gene on Chromosome 2 (mouse) and Chromosome 10 (human), respectively (http://www.ncbi.nlm.nih.gov/Genomes/). In the zebrafish genomic sequence assembly (http://www.ensembl.org/Danio_rerio/), we found a zebrafish homolog of STAM (ENSDARG00000002127) located on the same contig (CT027716.7) containing *cacnb2a*. This genomic synteny suggests that *cacnb2a* is an ortholog of mammalian *CACNB2*. We did not obtain sufficient syntenic information for *cacnb2b* because the genomic region containing *cacnb2b* is poorly assembled in the genomic database but the high level of sequence homology (63.9% identity) between CAB2b.1 and CAB2a suggests that *cacnb2b* is also an ortholog of mammalian *CACNB2*.

cacnb2a was expressed prominently by the trigeminal ganglia and the epiphysis at 24 hours post fertilization (hpf; Fig. 2B,C). At 48 hpf, *cacnb2a* expression in the brain increased with notable expression in the optic stalk (Fig. 2D). At 72 hpf, *cacnb2a* was still detectable in the epiphysis and was strongly expressed in the retina (Fig. 2E). No expression of *cacnb2a* was detected in the spinal cord from 24 hpf to 72 hpf (not shown).

cacnb2b was expressed extensively throughout the brain at higher levels compared with *cacnb2a* as well as in the spinal cord at 24 hpf (Fig. 2F,G). The expression of *cacnb2b* increased in the brain by 48 hpf (Fig. 2H,I) and remained high at 72 hpf (Fig. 2J). In addition to the CNS, there was weaker expression of *cacnb2b* in the olfactory placodes (Fig. 2F,H).

In mammals the VGCC β2 subunit is expressed in many tissues including heart, brain, lung, kidney, and pancreas (Hullin et al., 1992; Perez-Reyes et al., 1992). β2 is the predominant β subunit in the heart and targeted knockout of β2 results in prenatal death due to cardiac failure in mice (Ball et al., 2002). During embryonic development of the rat, however, β2 subunit in not detected in the heart until fetal day 15 and its abundance increases steadily with the maturation of the heart until birth (Haase et al., 2000). Similarly, as assayed by in situ hybridization expression of neither *cacnb2a* nor *cacnb2b* was detected in the developing cardiac tissue during the earliest stages of heart development in zebrafish.

Zebrafish *cacnb3a* and *cacnb3b*

The zebrafish *cacnb3a* gene was identified from genomic contig CR936486.7 in the Zv7 genome assembly. The cDNA (Genbank accession no. DQ372946) cloned by RT-PCR encodes a protein of 439 amino acids (CAB3a) that is most closely related to mammalian CAB3 (60% similarity; Fig. 3A). However, CAB3a has a shorter C-terminal domain than human and mouse CAB3 and could represent a splice variant of *cacnb3a*. *cacnb3a* was mapped by radiation-hybrid mapping to Chromosome 23, 5.23 cR from EST marker fd02b09 (LOD = 18.0).

cacnb3b was identified from genomic contig CT573349.6. The partial cDNA (GenBank accession no. DQ372947) cloned by RT-PCR encoded for 332 amino acid protein (CAB3Lb). The predicted protein sequence shared 55% similarity with human CAB3 and 72% similarity with zebrafish CAB3a. The nucleotide sequence identity between *cacnb3a* and *cacnb3b* was 79.8%, suggesting they were duplicated genes. *cacnb3b* was mapped to chromosome 23, 10.09 cR from SSLP marker Z13363 (LOD = 10.9), approximately 85.16 cR from *cacnb3a*.

Although the D3 region is variable among the β subunits, a highly conserved motif (AKQKQKQ/S/V) within D3 is found in neuronal β1, β3, and β4 but not in β2 (Dolphin, 2003). We found this conserved motif is also present in both zebrafish CAB3a and CAB3b (Fig. 3A).

Synteny between the region of mammalian and zebrafish genomes containing VGCCβ3 suggests that zebrafish *cacnb3a* and *cacnb3b* are orthologs of mammalian *CACNB3*. Mouse and human *CACNB3* are closely linked to adenylate cyclase 6 (*ADCY6*), DEAD polypeptide 23 (*DDX23*) and Rho family GTPase 1 (*RND1*). Zebrafish *cacnb3a* is found in the contig located in chromosome 23 containing zebrafish homolog of *ADCY6* (ENSDARG00000010558) and *DDX23* (ENSDARG00000021945). The *cacnb3b* is also found closely linked to another zebrafish homolog of *ADCY6* (ENSDARG00000027797) and a *RND1* homolog (ENSDARG00000004218) in chromosome 23. The synteny thus suggests that *cacnb3a* and *cacnb3b* may be duplicated orthologs of mammalian *CACNB3*.

At 24 hpf, *cacnb3a* was expressed in two groups of cells located in the forebrain immediately adjacent to the olfactory placodes (Fig. 3B). In the hindbrain, it was expressed by rhombomerically distributed pairs of cells that were likely to be reticulospinal neurons (Fig. 3C). In the spinal cord, *cacnb3a* was expressed by large, dorsally located cells likely to be mechanosensory Rohon-Beard neurons. In addition, *cacnb3a* expression was also detected in segmentally distributed neurons with ventrally projecting axons. These neurons are ventral to the Rohon-Beard neurons and likely to represent commissural neurons in the dorsal spinal cord (Kuwada et al., 1990; Fig. 3D). By 48 hpf, *cacnb3a* was expressed in the brain (Fig. 3E) with high levels of expression in groups of cells in the hindbrain (Fig. 3F), the trigeminal ganglion and the posterior lateral line ganglion (Fig. 3G). At 72 hpf, *cacnb3a* was expressed throughout the brain and in the trigeminal and other cranial sensory neurons (Fig. 3H).

At 24 hpf, expression of *cacnb3b* could be detected in the trigeminal ganglia, two groups of sensory neurons in the otic vesicles (Fig. 3I) and Rohon-Beard neurons in the dorsal spinal cord (Fig. 3J). By 48 hpf *cacnb3b* was detected in the retina, the trigeminal ganglia, the otocysts and the posterior lateral line ganglia (Fig. 3K). Sections showed that *cacnb3b* was expressed by cells in the otocyts at 72 hpf (Fig. 3L). Thus,

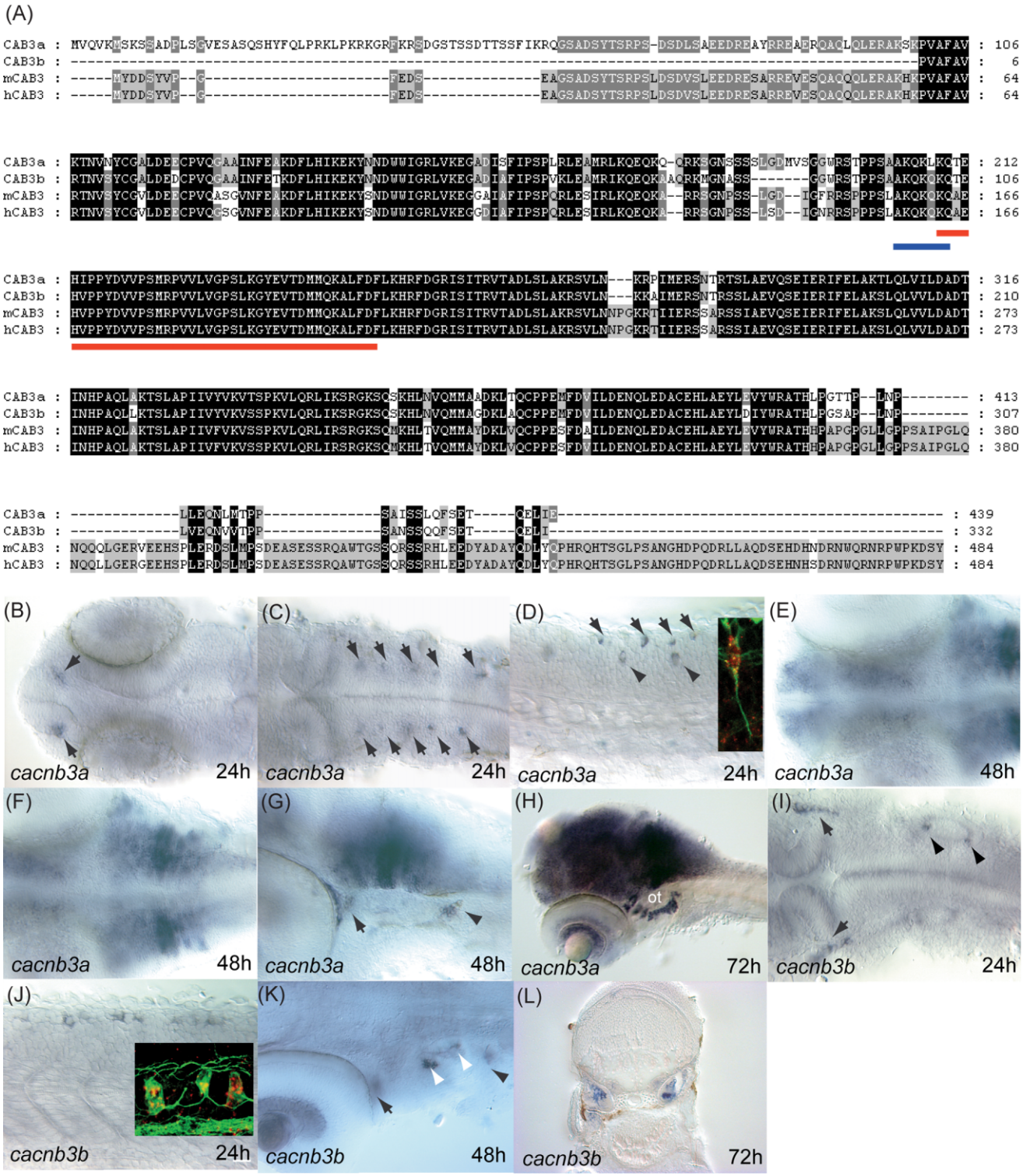

Fig. 3. Zebrafish *cacnb3a* and *cacnb3b* genes. **A:** Alignment of proteins encoded by zebrafish and mammalian *CACNB3* genes shows that they are highly homologous to each other. The red bar underlines the β interaction domain (BID). The blue bar underlines the AKQKQKQ/S/V motif that is conserved in β1, β3, and β4. **B:** Dorsal view of the head showing that *cacnb3a* is expressed in two groups of cells (arrows) in the forebrain adjacent to the olfactory placodes at 24 hpf. **C:** Dorsal view of the hindbrain showing the expression of *cacnb3a* in discrete bilateral groups of cells (arrows) that may represent reticulospinal neurons at 24 hpf. **D:** Lateral view of the spinal cord showing *cacnb3a* is expressed in cells in the dorsal cord likely to be Rohon-Beard neurons (arrows) and commissural neurons (arrowheads) at 24 hpf. Inset from of an embryo labeled with the *cacnb3a* riboprobe (red) and anti–acetylated-α-tubulin (green) showing a *cacnb3a*-expressing commissural neuron extending a ventrally-directed axon. **E:** Dorsal perspective of the head showing *cacnb3a* is expressed diffusely in the brain at 48 hpf. **F:** Dorsal view of the hindbrain showing that at 48 hpf *cacnb3a* is strongly expressed by discrete groups of cells in rhombomeres 4-6 based upon the location of the otocyst. **G:** Lateral view of the hindbrain showing expression of *cacnb3a* in the trigeminal ganglion (arrow) and posterior lateral line ganglion (arrowhead) as well as the cells in rhombomeres at 48 hpf. **H:** Lateral view of 72 hpf embryo showing strong expression of *cacnb3a* in the brain, the retina and the cells ventral to the otocyst (ot). **I:** Dorsal view of the hindbrain at 24 hpf showing *cacnb3b* expression in the trigeminal ganglion (arrows) and in two groups of cells likely to be sensory neurons in the otic vesicle (arrowheads). **J:** Lateral view of trunk at 24 hpf showing *cacnb3b* expression in dorsal cells likely to be Rohon-Beard neurons in the spinal cord. Inset from an embryo labeled with the riboprobe for *cacnb3b* (red) and anti–acetylated-α-tubulin (green) showing that the dorsal cells express *cacnb3b* and extend longitudinal axons in the dorsal spinal cord consistent with them being Rohon-Beard neurons. **K:** Dorsal view at 48 hpf showing *cacnb3b* expression in the retina, trigeminal ganglion (arrow), otic cells (white arrowhead) and posterior lateral line ganglion (black arrowhead). **L:** Transverse section of 96 hpf embryo showing *cacnb3* expression within the otocysts. Anterior is left in (B–K).

cacnb3b was expressed mainly by sensory neurons.

The mammalian *CACNB3* gene is mainly expressed in the brain but also in a variety of other tissues, including the aorta, trachea, lung, heart, pancreas, and adrenal gland (Hullin et al., 1992; Castellano et al., 1993). *CACNB3* knockout mice displayed reduced nociception (Murakami et al., 2002), which was attributed to the reduction of high voltage-gated Ca^{2+} currents in dorsal root ganglion cells. A similar reduction of voltage-gated Ca^{2+} currents was also observed in sympathetic neurons in *CACNB3* knockout mice (Namkung et al., 1998). Thus, *CACNB3* plays essential roles in the nervous system. The expression patterns of the two zebrafish *CACNB3* homologs are consistent with the functional studies in mammals. Furthermore, the expression patterns of *cacnb3a* and *cacnb3b* are partially overlapping. Both genes are expressed in mechanosensory neurons, such as Rohon-Beard neurons, trigeminal ganglion, and posterior lateral line ganglion neurons. Therefore, the two genes could act redundantly in these sensory neurons. However, *cacnb3a* but not *cacnb3b* is strongly expressed in the brain and some interneurons in the dorsal spinal cord, while *cacnb3b* is expressed in otic sensory cells. The diverged expression may allow for the analysis of *CACNB3* function in different sets of neurons. Zebrafish mutant *gemini* displays auditory–vestibular defects due to a mutation in *Cav1.3a*, which encodes an L-type VGCC α subunit localized at the ribbon synapses of inner ear hair cells (Sidi et al., 2004). It would be interesting to investigate whether CAB3b is preferentially associated with Cav 1.3a channels and facilitates its function in the neurons in inner ears.

Zebrafish *cacnb4a* and *cacnb4b*

Our database search yielded two *CACNB4* homologs in zebrafish. *cacnb4a* was initially identified from genomic contig BX548038.9 and the full-length cDNA (GenBank accession no. DQ372948) was cloned by RT-PCR. The predicted *cacnb4a* gene product (CAB4a) consists of 485 amino acids that shares 94% similarity with human CAB4 (Fig. 4A). Two cDNA clones (GenBank accession no. BQ260456 and CK362454) were first identified for *cacnb4b* and the genomic sequence of this gene was located in genomic contig BX072556.9. The cDNA cloned by RT-PCR (GenBank accession no. DQ372949) encoded for a protein of 489 amino acids (CAB4b) that was most homologous with human CAB4 (88% similarity; Fig. 4A). Previous structural analyses have shown that the D1 domain of the β4 subunit was unique compared with the D1 domains of the other VGCC β subunits (Vendel et al., 2006). This β4-specific D1 domain and the AKQKQKQ/S/V motif were found in both CAB4a and CAB4b (Fig. 4A).

We mapped *cacnb4a* to Chromosome 9, 30.11 cR from SSLP marker Z1273 (LOD = 12.0) and *cacnb4b* to Chromosome 6, 4.81 cR from EST marker fb33h05 (LOD = 15.9). The genomic regions containing *CACNB4* in mouse and human were highly syntenic. In these regions at least 7 genes (*NMI*, *TNFAIP6*, *RIF1*, *NEB*, *ARL5A*, *CACNB4*, and *STAM2*) are clustered in identical order on mouse Chromosome 2 and human Chromosome 2. We found a predicted zebrafish *STAM2* homolog (ENSDARG00000005318) located immediately adjacent to *cacnb4a* in the Zv6 genome assembly. Thus the synteny corroborated the assignment of *cacnb4a* as a *CACNB4* ortholog.

cacnb4a and *cacnb4b* were widely expressed in the CNS from 24 to 72 hpf. At 24 hpf, *cacnb4b* appeared to be expressed at higher levels in the brain compared with *cacnb4a* as assayed by in situ hybridization (Fig. 4B,C,H,I), but by 48 hpf expression of the two genes were quite similar (Fig. 4E,J). At 72 hpf, expression of *cacnb4a* was strong in the retina and various clusters of cells in the brain (Fig. 4F) while expression of *cacnb4b* was strong in the retina and presumptive cerebellum (Fig. 4K) as well as in segmentally distributed cells in the spinal cord (Fig. 4L). Beyond these differences a major distinction between *cacnb4a* and *cacnb4b* was that *cacnb4a* but not *cacnb4b* was expressed in the developing cardiac tube (Fig 4B).

Mouse *CACNB4* is expressed extensively in brain with prominent expression in the cerebellum (Castellano et al., 1993). *CACNB4* is essential for the function of neural circuits controlling motor behaviors because it is mutated in mouse *lethargic* mutants that exhibit an epilepsy-like phenotype (Burgess et al., 1997; Haase et al., 2000). Both zebrafish *CACNB4* homologs are expressed widely in brain, consistent with the neural function of *CACNB4*. We detected a high level of *cacnb4b* transcript in the cerebellum in accordance with a role for *CACNB4b* in regulating motor behaviors. The β4 subunit is also expressed by the fetal heart in rats and precedes expression of the β2 subunit (Haase et al., 2000). Similarly in zebrafish *cacnb4a* was expressed by the embryonic heart during 24–72 hpf when neither *cacnb2a* nor *cacnb2b* expression was detected. Together, these data suggest that both zebrafish *cacnb4a* and *cacnb4b* are orthologs of mammalian *CACNB4*.

Expression of VGCC β Subunits in Zebrafish Retina

The zebrafish retina as with the other vertebrate retinas consists of three main layers: the ganglion cell layer (GCL) adjacent to the lens, the inner nuclear layer (INL) and the photoreceptors (PR; Pujic and Malicki, 2004). In the zebrafish retina, the *CACNB* family genes are expressed in distinct patterns during embryonic development. *cacnb2a* expression is barely detectable at 48hpf (Fig. 2D), but by 96 hpf, it is specifically expressed in photoreceptors and the outermost half of INL while absent in the GCL and the innermost tier of INL (Figs. 2E, 5A). In contrast, *cacnb2b* expression in the retina was detectable as early as 24 hpf (Fig. 2F). After 48 hpf, *cacnb2b* is strongly expressed in the ganglion cell layer in addition to its weak and diffused expression in the INL (Figs. 2H,J, 5B). The two *CACNB3* homologs exhibited partially overlapping expression patterns. At 72 and 96 hpf, both *cacnb3a* and *cacnb3b* were expressed in the GCL with additional expression of *cacnb3a* in the innermost tier of the INL that is immediately adjacent to the inner plexiform layer (Figs. 3G, M, 5C,D). The expression of the two *CACNB4* homologs also appeared to be partially overlapping. *cacnb4a* expression in retina

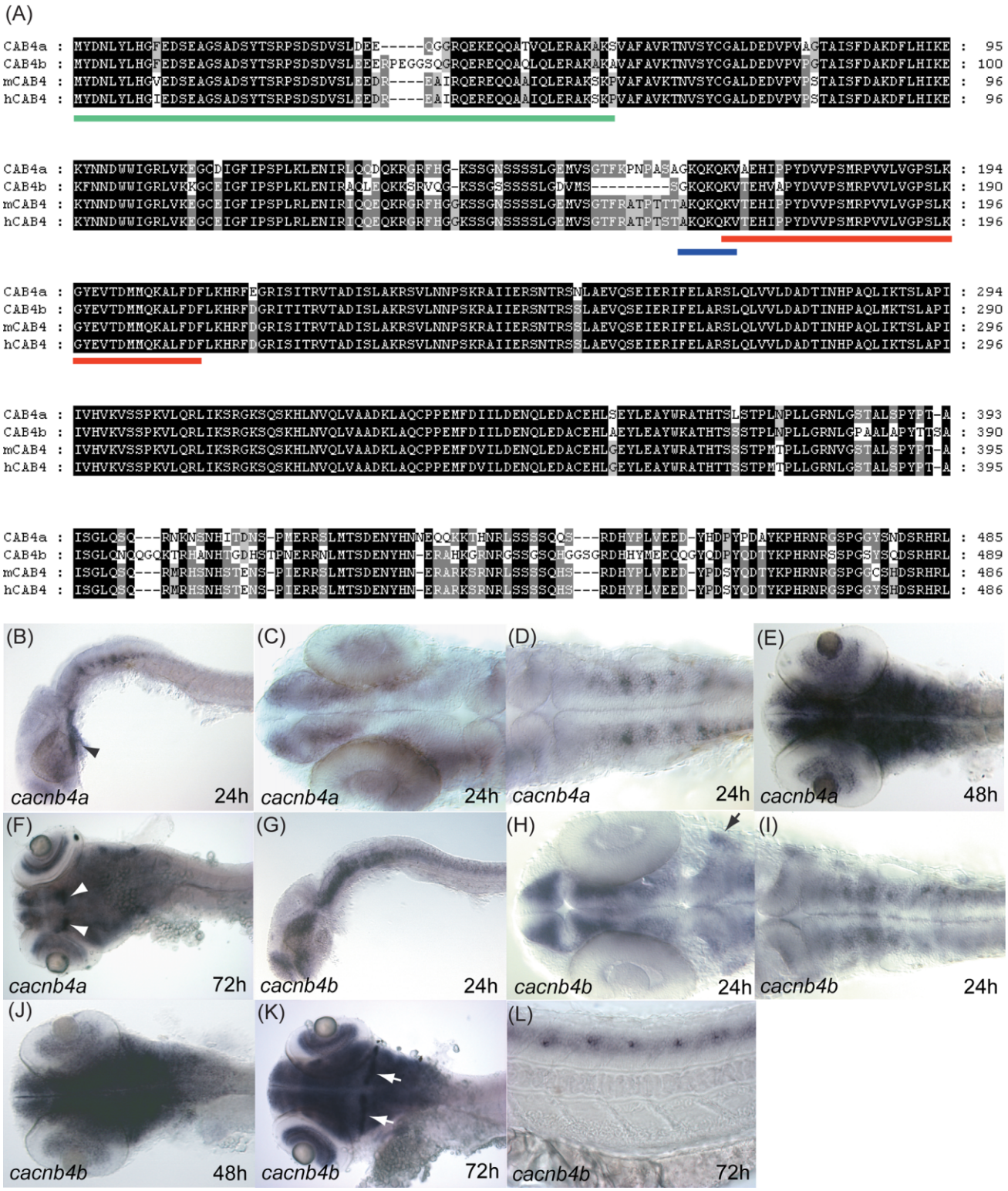

Fig. 4. Zebrafish *cacnb4a* and *cacnb4b* genes. **A:** Alignment of protein sequences encoded by zebrafish and mammalian *CACNB4* genes shows that they are highly homologous to each other. The red bar underlines the β interaction domain (BID). The blue bar underlines the AKQKQKQ/S/V motif that is conserved in β1, β3 and β4. The green bar underlines the β4-specific D1 domain. **B:** Lateral view showing *cacnb4a* expression in the brain and the cardiac tube (arrow) at 24 hpf. **C:** Dorsal view showing expression of *cacnb4a* in the forebrain, retina, and midbrain at 24 hpf. **D:** Dorsal view showing *cacnb4a* is expressed in the hindbrain and spinal cord at 24 hpf. **E:** Dorsal view showing *cacnb4* is expressed strongly in the brain at 48 hpf. **F:** Dorsal view of 72 hpf embryos showing *cacnb4a* expression in the brain. The white arrowheads indicate the two groups of cells in the dorsal midbrain with strong expression of *cacnb4a*. **G:** Lateral view showing *cacnb4b* is expressed in the brain and spinal cord at a higher level than *cacnb4a* at 24hpf. Note *cacnb4b* is not detected in the cardiac tube. **H:** Dorsal view of the hindbrain showing *cacnb4b* is strongly expressed in the forebrain, midbrain, and trigeminal ganglia (arrow) at 24 hpf. **I:** Dorsal view showing *cacnb4b* is expressed in hindbrain and spinal cord at 24 hpf. **J:** Dorsal view showing strong expression of *cancb4b* in the brain at 48 hpf. **K:** Dorsal view of 72 hpf embryo showing expression of *cacnb4b* persists in the brain. The white arrows indicate stronger expression of *cacnb4b* in the cerebellum compared with the rest of the brain. **L:** Lateral view at 72 hpf showing expression of *cacnb4b* by periodically located cells in the spinal cord. Anterior is left in all the panels.

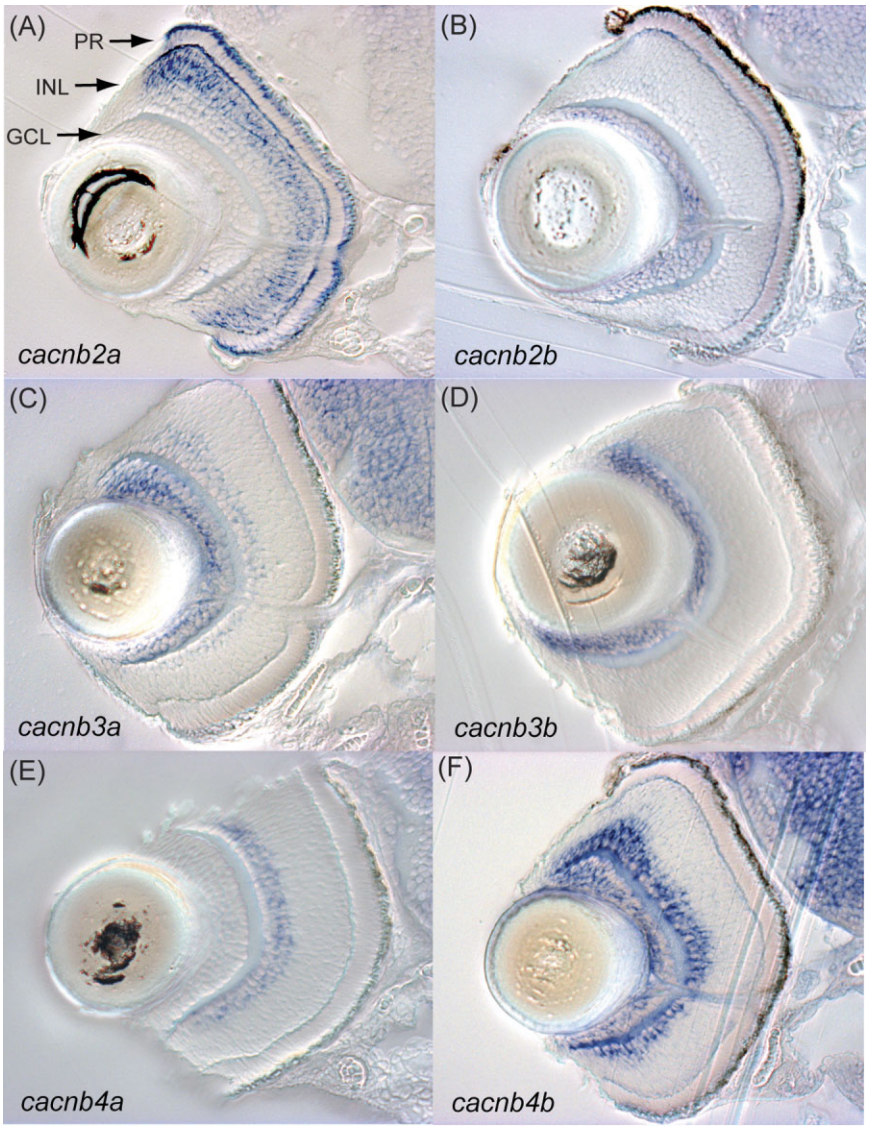

Fig. 5. Expression of *cacnb* genes in zebrafish retina at 96 hpf. Transverse sections indicate that zebrafish *cacnb* genes are expressed in distinct regions in the retina at 96 hpf. **A:** *cacnb2a* is expressed in the outermost inner nuclear layer (INL) and by photoreceptors (PR). **B:** *cacnb2b* is expressed in the ganglion cell layer (GCL). **C:** *cacnb3a* is expressed in GCL and the innermost INL. **D:** *cacnb3b* is expressed exclusively in the GCL. **E:** *cacnb4a* is expressed only in the innermost INL. **F:** *cacnb4b* is expressed in GCL and the innermost INL.

was restricted to the innermost tier of the INL (Fig. 5E) while *cacnb4b* was expressed in this region as well as the GCL (Fig. 5F). Interestingly, *cacnb3a* and *cacnb4b* were expressed in a similar pattern that was complementary to that of *cacnb2a*.

In mice, the β2 subunit is essential for the retinal formation. Knocking out β2 in the CNS leads to impaired vision, abnormal ERGs and morphological defects in the outer plexiform layer (Ball et al., 2002). Moreover, the expression of VGCC α1F in the outer segment (photoreceptor) of retina is abolished in these mutant mice. On the other hand, CNS knock-out of β1, β3, and β4 does not produce any obvious abnormality in the eye. Our results indicate that in the zebrafish retina the photoreceptors and the outermost layer of the INL express only the two β2 subunits while the other regions express multiple β subunits, suggesting that in the GCL and the inner layer of the INL these β subunits could function redundantly. This expression pattern is consistent with the loss of α1F expression in mice deficient for β2 in photoreceptors while there was little abnormality in mice deficient for the other β subunits.

Of the VGCC β subunits, *cacnb1* appears to be the only one expressed in skeletal muscle in zebrafish (Table 1). This is consistent with the muscle phenotype found in *relaxed* mutants that is due to loss-of-function mutations in *CACNB1*(Schredelseker et al., 2005; Zhou et al., 2006). Of interest, *CACNB1* is also expressed throughout the CNS, including the hindbrain and spinal cord, yet spinal motor output following tactile stimulation of mutants is normal. Because the hindbrain and spinal cord are sufficient for motor responses to tactile stimuli, normal neural responsiveness of *relaxed* mutants suggests that these regions of the CNS function normally despite the loss of *cacnb1*. The normal response of the CNS to tactile stimulation in *relaxed* mutants could be due to the redundant actions of the other six *CACNB* genes, which are also extensively expressed in the nervous system including the hindbrain and spinal cord. Additionally, a duplicate *cacnb1* might also act redundantly. At present, neither genome database searches nor degenerate PCR targeting the β1-specific domain produced any sequence other than the known *cacnb1* gene (data not shown) suggesting a lack of duplication of *cacnb1* in zebrafish. It is notable that we were able to identify only one *cacnb1* gene in *Takifugu rubripes* genome as well, which suggests that there may not be a duplication of *CACNB1* in teleosts. However, because the zebrafish genome has not been completely assembled, we cannot rule out that a duplicate *cacnb1* might exist.

The zebrafish VGCC β subunit homologs are similar with their mammalian counterparts in sequence, genomic synteny, and expression pattern. Yet significant divergence of this gene family exists in zebrafish. With the possible exception of β1, the other β subunits appear to have undergone gene duplication and specification during evolution, as each pair of putative duplicates share significant sequence similarity but only partially overlapping expression patterns. The expression of the duplicates in different cells may be useful for revealing the specific function of *CACNB* genes

Developmental Dynamics

TABLE 1. Expression Patterns of Mammalian CACNB Genes and Zebrafish Homologs

Mammalian Gene	Mammalian expression patterns[a]	Zebrafish homolog	Chromosomal locus	Zebrafish protein	Embryonic expression in zebrafish
CACNB1	Skeletal muscle (β1a)[1,2] , neurons (β1b)[3]	*cacnb1*	Chr3 LOD=9.3	CAB1a (517aa) CAB1c (603aa)	Skeletal muscle, brain, spinal cord, trigeminal ganglia, olfactory placodes[4]
CACNB2	Heart, brain, aorta, lung, kidney, pancreas[5-7]	*cacnb2a*	Chr2 LOD=10.8	CAB2a (377aa)	brain, spinal cord, trigeminal ganglia, optic stalks, retina (inner nuclear layer, photoreceptor)
		cacnb2b	Chr7 LOD=16.5	CAB2a.1 (598aa) CAB2b.2 (37aa)	brain, spinal cord, retina (ganglion cell layer), olfactory placodes
CACNB3	Brain, aorta, trachea, lung, heart, pancreas, adrenal gland[8-11]	*cacnb3a*	Chr23 LOD=18.0	CAB3a (439aa)	brain, spinal interneurons, Rohon-Beard neurons, retina (ganglion cell layer, inner nuclear layer)
		cacnb3b	Chr23 LOD=12.4	CAB3b (322aa, partial)	trigeminal ganglia, retina (ganglion cell layer, inner nuclear layer), Rohon-Beard neurons, otic cells
CACNB4	Brain (predominantly in cerebellum), kidney[12,13]	*cacnb4a*	Chr9 LOD=12.0	CAB4a (485aa)	brain, spinal cord, heart, retina (inner nuclear layer)
		cacnb4b	Chr6 LOD=15.9	CAB4b (489aa)	brain, spinal cord, trigeminal ganglia, retina (ganglion cell layer, inner nuclear layer)

[a]References are as follows: 1: Powers et al., 1992; 2, Ruth et al., 1989; 3: Pragnell et al., 1991; 4: Zhou et al., 2006; 5: Hullin et al., 1992; 6: Perez-Reyes et al., 1992; 7: Massa et al., 1995; 8:Hullin et al., 1992; 9: Castellano et al., 1993a; 10: Collin et al., 1994; 11: Murakami et al., 1996; 12: Castellano et al., 1993b; 13: Burgess et al., 1997.

in the cells that selectively express each of the duplicates.

EXPERIMENTAL PROCEDURES

Fish Breeding and Maintenance

Zebrafish (*Danio rerio*) were bred and maintained in a breeding facility following established procedures that meet the guidelines set forth by the University of Michigan Animal Care and Use protocols. Embryos were collected after natural spawns, kept at 28.5°C, and staged according to hours post fertilization (hpf; Westerfield, 1995).

Database Search

A BLAST search for zebrafish *CACNB* gene homologs was done using the sequence of zebrafish *CACNB1c* (GenBank accession no. DQ198172). The GenBank database was searched for EST clones and the zebrafish genome database (http://www.ensembl.org/Danio_rerio/) for genomic sequences. Each EST clone was completely sequenced to determine whether it contained a complete open reading frame. The acquired genomic sequences were analyzed with Genscan software (http://genes.mit.edu/GENSCAN.html) to determine potential exons, which were used to design primers for RT-PCR.

RT-PCR and Cloning

Total RNA was isolated from 24 to 30 hpf embryos by using Tri-reagent (Invitrogen, Carlsbad, CA) and reverse-transcribed with oligo dT primers and Superscript II reverse transcriptase (Invitrogen) following the manufacturer's instructions (Superscript II manual, version 11-11-203). The PCR products were gel-purified, cloned into the pGEM T-easy vector (Promega, Madison, WI) and sequenced at the University of Michigan Sequencing Core. Sequence alignment (Clustal W method) and construction of phylogenetic tress (unrooted) were done with the Lasergene software (DNAStar, Madison, WI). The neuronal isoform of *cacnb1* (CAB1c) was included as an outgroup in the phylogenetic analysis. The length of each pair of branches represents the distance between sequence pairs, while the units at the bottom of the tree indicate the number of substitution events. The dotted lines indicate the negative length of branches.

Developmental Dynamics

For degenerate RT-PCR of *CACNB1* gene, the following primers were used for the amplification of β1-specific D2-D4 domain: forward primer, 5′-CCACCTCCAACTCCTTCGTNMGNCARGG, reverse primer, 5′-CATGGTCCGGTTCAGCARNGGRTTNGG. Other RT-PCR Primer sequences are available upon request to the authors.

In Situ Hybridization and Sectioning

In situ hybridization was carried out following standard protocols (Li et al., 2004). To prevent pigmentation after 24 hpf, embryos were transferred to water containing 0.2 mM of 1-phenyl-2-thiourea at 20 hpf and fixed at appropriate stages. The antisense digoxigenin (DIG) -labeled probes for zebrafish *CACNB* genes were synthesized in vitro from the cloned cDNA sequences. The sense probes were used as negative controls and produced no significant signals (not shown). In some cases, after in situ hybridization, embryos were washed in phosphate buffered saline, dehydrated with 25%, 50%, 75%, 85%, 95%, and 100% ethanol and embedded in JB-4 plastics (Polysciences). Sectioning was performed with a Leica RM2265 automatic microtome. For double labeling, in situ hybridization was carried out using Fast Red (Roche Applied Science) as a coloration substrate, followed by immunohistochemical labeling with anti-acetylated tubulin antibody (1:500; Sigma) and secondary anti-mouse IgG (1:2,000; Molecular Probes). Fluorescence imaging was acquired with a Leica SP5 confocal microscope.

Radiation Hybrid Mapping

The LN54 radiation hybrid panel was used for physical mapping of zebrafish sequences (Hukriede et al., 1999). Mapping primers were designed according to the genomic sequence information acquired by searching the zebrafish genome database. Primer sequences are available upon request to the authors.

REFERENCES

Ball SL, Powers PA, Shin HS, Morgans CW, Peachey NS, Gregg RG. 2002. Role of the beta(2) subunit of voltage-dependent calcium channels in the retinal outer plexiform layer. Invest Ophthalmol Vis Sci 43:1595–1603.

Beurg M, Sukhareva M, Ahern CA, Conklin MW, Perez-Reyes E, Powers PA, Gregg RG, Coronado R. 1999. Differential regulation of skeletal muscle L-type Ca2+ current and excitation-contraction coupling by the dihydropyridine receptor beta subunit. Biophys J 76:1744–1756.

Bichet D, Cornet V, Geib S, Carlier E, Volsen S, Hoshi T, Mori Y, De Waard M. 2000. The I-II loop of the Ca2+ channel alpha1 subunit contains an endoplasmic reticulum retention signal antagonized by the beta subunit. Neuron 25:177–190.

Birnbaumer L, Qin N, Olcese R, Tareilus E, Platano D, Costantin J, Stefani E. 1998. Structures and functions of calcium channel beta subunits. J Bioenerg Biomembr 30:357–375.

Brosenitsch TA, Salgado-Commissariat D, Kunze DL, Katz DM. 1998. A role for L-type calcium channels in developmental regulation of transmitter phenotype in primary sensory neurons. J Neurosci 18:1047–1055.

Burgess DL, Jones JM, Meisler MH, Noebels JL. 1997. Mutation of the Ca2+ channel beta subunit gene Cchb4 is associated with ataxia and seizures in the lethargic (lh) mouse. Cell 88:385–392.

Castellano A, Wei X, Birnbaumer L, Perez-Reyes E. 1993a. Cloning and expression of a neuronal calcium channel beta subunit. J Biol Chem 268:12359–12366.

Castellano A, Wei X, Birnbaumer L, Perez-Reyes E. 1993b. Cloning and expression of a third calcium channel beta subunit. J Biol Chem 268:3450–3455.

Castellano A, Wei X, Birnbaumer L, Perez-Reyes E. 1993. Cloning and expression of a neuronal calcium channel beta subunit. J Biol Chem 268:12359–12366.

Catterall WA. 2000. Structure and regulation of voltage-gated Ca2+ channels. Annu Rev Cell Dev Biol 16:521–555.

Colecraft HM, Alseikhan B, Takahashi SX, Chaudhuri D, Mittman S, Yegnasubramanian V, Alvania RS, Johns DC, Marban E, Yue DT. 2002. Novel functional properties of Ca(2+) channel beta subunits revealed by their expression in adult rat heart cells. J Physiol 541:435–452.

Collin T, Lory P, Taviaux S, Courtieu C, Guilbault P, Berta P, Nargeot J. 1994. Cloning, chromosomal location and functional expression of the human voltage-dependent calcium-channel beta 3 subunit. Eur J Biochem 220:257–262.

Dolphin AC. 2003. Beta subunits of voltage-gated calcium channels. J Bioenerg Biomembr 35:599–620.

Haase H, Pfitzmaier B, McEnery MW, Morano I. 2000. Expression of Ca(2+) channel subunits during cardiac ontogeny in mice and rats: identification of fetal alpha(1C) and beta subunit isoforms. J Cell Biochem 76:695–703.

Herlitze S, Xie M, Han J, Hummer A, Melnik-Martinez KV, Moreno RL, Mark MD. 2003. Targeting mechanisms of high voltage-activated Ca2+ channels. J Bioenerg Biomembr 35:621–637.

Hukriede NA, Joly L, Tsang M, Miles J, Tellis P, Epstein JA, Barbazuk WB, Li FN, Paw B, Postlethwait JH, Hudson TJ, Zon LI, McPherson JD, Chevrette M, Dawid IB, Johnson SL, Ekker M. 1999. Radiation hybrid mapping of the zebrafish genome. Proc Natl Acad Sci U S A 96:9745–9750.

Hullin R, Singer-Lahat D, Freichel M, Biel M, Dascal N, Hofmann F, Flockerzi V. 1992. Calcium channel beta subunit heterogeneity: functional expression of cloned cDNA from heart, aorta and brain. EMBO J 11:885–890.

Komuro H, Rakic P. 1992. Selective role of N-type calcium channels in neuronal migration. Science 257:806–809.

Kuwada JY, Bernhardt RR, Chitnis AB. 1990. Pathfinding by identified growth cones in the spinal cord of zebrafish embryos. J Neurosci 10:1299–1308.

Leclerc C, Duprat AM, Moreau M. 1995. In vivo labelling of L-type Ca2+ channels by fluorescent dihydropyridine: correlation between ontogenesis of the channels and the acquisition of neural competence in ecotderm cells from Pleurodeles waltl embryos. Cell Calcium 17:216–224.

Leclerc C, Daguzan C, Nicolas MT, Chabret C, Duprat AM, Moreau M. 1997. L-type calcium channel activation controls the in vivo transduction of the neuralizing signal in the amphibian embryos. Mech Dev 64:105–110.

Leclerc C, Webb SE, Daguzan C, Moreau M, Miller AL. 2000. Imaging patterns of calcium transients during neural induction in Xenopus laevis embryos. J Cell Sci 113(pt 19):3519–3529.

Li Q, Shirabe K, Kuwada JY. 2004. Chemokine signaling regulates sensory cell migration in zebrafish. Dev Biol 269:123–136.

Massa E, Kelly KM, Yule DI, MacDonald RL, Uhler MD. 1995. Comparison of fura-2 imaging and electrophysiological analysis of murine calcium channel alpha 1 subunits coexpressed with novel beta 2 subunit isoforms. Mol Pharmacol 47:707–716.

Moorman SJ, Hume RI. 1993. Omega-conotoxin prevents myelin-evoked growth cone collapse in neonatal rat locus coeruleus neurons in vitro. J Neurosci 13:4727–4736.

Moreau M, Leclerc C, Gualandris-Parisot L, Duprat AM. 1994. Increased internal Ca2+ mediates neural induction in the amphibian embryo. Proc Natl Acad Sci U S A 91:12639–12643.

Murakami M, Fleischmann B, De Felipe C, Freichel M, Trost C, Ludwig A, Wissenbach U, Schwegler H, Hofmann F, Hescheler J, Flockerzi V, Cavalie A. 2002. Pain perception in mice lacking the beta3 subunit of voltage-activated calcium channels. J Biol Chem 277:40342–40351.

Murakami M, Wissenbach U, Flockerzi V. 1996. Gene structure of the murine calcium channel beta3 subunit, cDNA and characterization of alternative splicing

and transcription products. Eur J Biochem 236:138–143.

Namkung Y, Smith SM, Lee SB, Skrypnyk NV, Kim HL, Chin H, Scheller RH, Tsien RW, Shin HS. 1998. Targeted disruption of the Ca2+ channel beta3 subunit reduces N- and L-type Ca2+ channel activity and alters the voltage-dependent activation of P/Q-type Ca2+ channels in neurons. Proc Natl Acad Sci U S A 95: 12010–12015.

Palma V, Kukuljan M, Mayor R. 2001. Calcium mediates dorsoventral patterning of mesoderm in Xenopus. Curr Biol 11: 1606–1610.

Perez-Reyes E, Castellano A, Kim HS, Bertrand P, Baggstrom E, Lacerda AE, Wei XY, Birnbaumer L. 1992. Cloning and expression of a cardiac/brain beta subunit of the L-type calcium channel. J Biol Chem 267:1792–1797.

Powers PA, Liu S, Hogan K, Gregg RG. 1992. Skeletal muscle and brain isoforms of a beta-subunit of human voltage-dependent calcium channels are encoded by a single gene. J Biol Chem 267: 22967–22972.

Pragnell M, Sakamoto J, Jay SD, Campbell KP. 1991. Cloning and tissue-specific expression of the brain calcium channel beta-subunit. FEBS Lett 291:253–258.

Pujic Z, Malicki J. 2004. Retinal pattern and the genetic basis of its formation in zebrafish. Semin Cell Dev Biol 15:105–114.

Qin N, Platano D, Olcese R, Stefani E, Birnbaumer L. 1997. Direct interaction of gbetagamma with a C-terminal gbetagamma-binding domain of the Ca2+ channel alpha1 subunit is responsible for channel inhibition by G protein-coupled receptors. Proc Natl Acad Sci U S A 94:8866–8871.

Rettig J, Heinemann C, Ashery U, Sheng ZH, Yokoyama CT, Catterall WA, Neher E. 1997. Alteration of Ca2+ dependence of neurotransmitter release by disruption of Ca2+ channel/syntaxin interaction. J Neurosci 17:6647–6656.

Rottbauer W, Baker K, Wo ZG, Mohideen MA, Cantiello HF, Fishman MC. 2001. Growth and function of the embryonic heart depend upon the cardiac-specific L-type calcium channel alpha1 subunit. Dev Cell 1:265–275.

Ruth P, Rohrkasten A, Biel M, Bosse E, Regulla S, Meyer HE, Flockerzi V, Hofmann F. 1989. Primary structure of the beta subunit of the DHP-sensitive calcium channel from skeletal muscle. Science 245:1115–1118.

Schredelseker J, Di Biase V, Obermair GJ, Felder ET, Flucher BE, Franzini-Armstrong C, Grabner M. 2005. The beta 1a subunit is essential for the assembly of dihydropyridine-receptor arrays in skeletal muscle. Proc Natl Acad Sci U S A 102:17219–17224.

Sheng ZH, Rettig J, Takahashi M, Catterall WA. 1994. Identification of a syntaxin-binding site on N-type calcium channels. Neuron 13:1303–1313.

Sidi S, Busch-Nentwich E, Friedrich R, Schoenberger U, Nicolson T. 2004. gemini encodes a zebrafish L-type calcium channel that localizes at sensory hair cell ribbon synapses. J Neurosci 24: 4213–4223.

Takahashi SX, Mittman S, Colecraft HM. 2003. Distinctive modulatory effects of five human auxiliary beta2 subunit splice variants on L-type calcium channel gating. Biophys J 84:3007–3021.

Vendel AC, Terry MD, Striegel AR, Iverson NM, Leuranguer V, Rithner CD, Lyons BA, Pickard GE, Tobet SA, Horne WA. 2006. Alternative splicing of the voltage-gated Ca2+ channel beta4 subunit creates a uniquely folded N-terminal protein binding domain with cell-specific expression in the cerebellar cortex. J Neurosci 26:2635–2644.

Walker D, De Waard M. 1998. Subunit interaction sites in voltage-dependent Ca2+ channels: role in channel function. Trends Neurosci 21:148–154.

Westerfield M. 1995. The zebrafish book. Eugene, OR: University of Oregon.

Zhou W, Saint-Amant L, Hirata H, Cui WW, Sprague SM, Kuwada JY. 2006. Non-sense mutations in the dihydropyridine receptor beta1 gene, CACNB1, paralyze zebrafish relaxed mutants. Cell Calcium 39:227–236.

Developmental Dynamics